ATMOSPHERIC SCIENCE LETTERS
Atmos. Sci. Let. **9**: 171–175 (2008)
Published online 16 June 2008 in Wiley InterScience
(www.interscience.wiley.com) **DOI:** 10.1002/asl.187

RMetS
Royal Meteorological Society

Vertically combined shaved cell method in a z-coordinate nonhydrostatic atmospheric model

Hiroe Yamazaki* and Takehiko Satomura
Division of Earth and Planetary Sciences, Graduate School of Science, Kyoto University, Sakyo, Kyoto, Japan

**Correspondence to:*
Hiroe Yamazaki, Division of Earth and Planetary Sciences, Graduate School of Science, Kyoto University, Sakyo, Kyoto, 606-8502, Japan.
E-mail: yamazaki_h@kugi.kyoto-u.ac.jp

Received: 23 January 2008
Revised: 22 April 2008
Accepted: 28 April 2008

Abstract

The vertically combined shaved cell method is implemented into a z-coordinate nonhydrostatic two-dimensional atmospheric model based on the finite-volume method. Quasi-flux form fully compressible equations are employed as governing equations. The results of flow over a bell-shaped mountain and a semicircular mountain are compared to those from a model using terrain-following coordinates. These results indicate that the proposed method does not suffer from vertical velocity errors at the edge of the cells, and reproduces smooth and accurate mountain waves over not only gentle but also steep slopes where significant errors are observed in the terrain-following model. Copyright © 2008 Royal Meteorological Society

Keywords: shaved cell method; nonhydrostatic atmospheric model; z-coordinate; high-resolution model; flux form equations

1. Introduction

Synchronizing with the rapid development of computer technology, resolutions of atmospheric numerical models have increased significantly. Today, horizontal grid intervals of a couple of kilometers are commonly used in research fields of local weather, and extremely high-resolution simulations, which use a few hundred meters horizontal grid intervals, should be possible within ten years. However, one hurdle to high-resolution simulations is the representation of topography because the commonly used terrain-following representation of topography induces large truncation errors over steep slopes (e.g. Thompson *et al*., 1985; Satomura, 1989). Because an increase in horizontal resolution introduces steep slopes over mountain areas, truncation errors will become more serious in high-resolution simulations. Thus, other representation methods of topography such as Cartesian coordinates are desirable for high-resolution models. Hereafter in this study, the Cartesian coordinate system is called the 'z-coordinate'.

Representations of complex topography in the z-coordinate are roughly grouped into three methods: box cell method, partial cell method, and shaved cell method. The box cell method has been used in both atmospheric and ocean models (e.g. Mesinger *et al*., 1988). Because the box cell method approximates topography as a step-like geometry fitted into model grids (Figure 1(a)), it represents steep slopes without distorting the vertical coordinates, but represents topography precisely only when the horizontal and vertical resolutions are so high that the height of one step is negligibly small. In addition, it is also noted that the step-like representation of topography introduces large errors into orographic gravity waves over a smooth topography (Gallus and Klemp, 2000). Hence, the partial cell method adjusts the thickness of the model cells abutting the earth surface (Figure 1(b)), and this method has used infinite-volume ocean models (e.g. Semtner and Mintz, 1977).

The shaved cell method, which was proposed and implemented into a finite-volume ocean model by Adcroft *et al*. (1997), cuts model cells by piecewise linear topography (Figure 1(c)). Adcroft *et al*. (1997) compared the shaved cell method, the partial cell method, and the box cell method, and demonstrated that the finite-volume representations of the shaved cell method and the partial cell method are clearly superior to the box cell representation. In particular, they concluded that the shaved cell method is the most conducive to smooth and accurate topography representation, although the partial cell method is a good compromise for shallow slopes. The shaved cell method has also been applied to an atmospheric model by Steppeler *et al*. (2002) and Steppeler *et al*. (2006). Steppeler *et al*. (2002) showed that the shaved cell method reproduces flow over a gently sloping bell-shaped mountain as precisely as a model using the terrain-following coordinates. In Steppeler *et al*. (2006), tests of precipitation forecasts over realistic mountains were performed using the shaved cell model, and compared with those using the terrain-following model. However, they did not clearly show if the shaved cell method is adaptive to steep mountains.

In this article, the shaved cell method is modified and applied to a nonhydrostatic model. It should be noted that in the shaved cell method, small cells cut by topography require small-time increments to satisfy the Courant–Friedrichs–Lewy (CFL) condition. Although Steppeler *et al*. (2002) used the

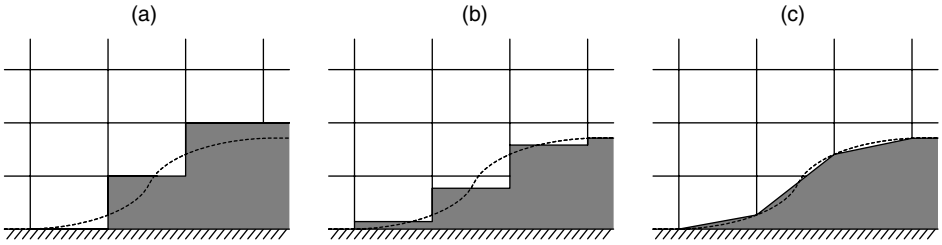

Figure 1. Three z-coordinate topography representations: (a) a box cell method, (b) a partial cell method, and (c) a shaved cell method. Solid lines and dashed lines describe the coordinates and real topography, respectively. Shaded regions describe the topographic representations in each model.

thin-wall approximation (Bonaventura, 2000) to avoid impractically small-time increments, we use another approach in which small cells are combined with upper cells to maintain the volume of cells larger than half a regular cell. This approach has been used in hydrodynamic models in the engineering field (e.g. Quirk, 1994), but is applied in this article to an atmospheric model to maintain reasonable conservation characteristics and computer resource consumption.

Quasi-flux form fully compressible dynamical equations developed by Satomura and Akiba (2003) are employed, because flux form equations are well suited to the finite-volume method in view of the conservation characteristics. Combining the vertically combined shaved cell (V-CSC) method and the quasi-flux form equation should result in high-resolution and highly precise simulations over complex terrain.

To verify the performance of the modified shaved cell method, the results of two-dimensional numerical simulations of flow over a mountain using the developed model will be compared to those from a terrain-following model. The model will be integrated not only over gentle slopes, but also steep slopes where terrain-following models induce large truncation errors.

2. Model description

The quasi-flux form fully compressible equations used in the present study are

$$\frac{\partial \rho u}{\partial t} = -\frac{\partial \rho u u}{\partial x} - \frac{\partial \rho u w}{\partial z} - \frac{\partial p'}{\partial x} \tag{1}$$

$$\frac{\partial \rho w}{\partial t} = -\frac{\partial \rho w u}{\partial x} - \frac{\partial \rho w w}{\partial z} - \frac{\partial p'}{\partial z} - \rho' g \tag{2}$$

$$\frac{\partial p'}{\partial t} = -\frac{c_p R}{c_v p_0}\left(\frac{p}{p_0}\right)^{R/c_p}\left(\frac{\partial \rho u \theta}{\partial x} + \frac{\partial \rho w \theta}{\partial z}\right) \tag{3}$$

$$\frac{\partial \rho'}{\partial t} = -\frac{\partial \rho u}{\partial x} - \frac{\partial \rho w}{\partial z} \tag{4}$$

$$p = \overline{p}_{(x,z)} + p'_{(x,z,t)} \tag{5}$$

$$\rho = \overline{\rho}_{(x,z)} + \rho'_{(x,z,t)} \tag{6}$$

$$\frac{\partial \overline{p}}{\partial z} = -\overline{\rho} g \tag{7}$$

where the variables are the standard definitions. This form was determined by Satomura and Akiba (2003), and has an advantage in that it does not suffer from the cancellation error because of subtracting the hydrostatic variable ($\overline{p}$ or $\overline{\rho}$) from the nearly hydrostatic total variable (p or ρ).

The shaved cell method approximates the topography by piecewise linear slopes as shown in Figure 2(a) where the scalar variables (p' and ρ') are defined at the scalar cells denoted by thick lines, while momenta (ρu and ρw) are defined at staggered cells. Descretized forms of Equations (1)–(4) are given using the notation of Arakawa and Lamb (1977):

$$\frac{\partial \rho u}{\partial t} = -\frac{\delta_x(\overline{L_x \rho u}^x \overline{u}^x)}{V_{\rho u}} - \frac{\delta_z(\overline{L_z \rho w}^x \overline{u}^z)}{V_{\rho u}} - \frac{\delta_x p'}{\Delta x} \tag{8}$$

$$\frac{\partial \rho w}{\partial t} = -\frac{\delta_x(\overline{L_x \rho u}^z \overline{w}^x)}{V_{\rho w}} - \frac{\delta_z(\overline{L_z \rho w}^z \overline{w}^z)}{V_{\rho w}} - \frac{\delta_z p'}{\Delta z} - \overline{\rho'}^z g \tag{9}$$

$$\frac{\partial p'}{\partial t} = -\frac{c_p R}{c_v p_0}\left(\frac{p}{p_0}\right)^{R/c_p}\left\{\frac{\delta_x(L_x \rho u \overline{\theta}^x)}{V_{p'}} + \frac{\delta_z(L_z \rho w \overline{\theta}^z)}{V_{p'}}\right\} \tag{10}$$

$$\frac{\partial \rho'}{\partial t} = -\frac{\delta_x(L_x \rho u)}{V_{p'}} - \frac{\delta_z(L_z \rho w)}{V_{p'}} \tag{11}$$

where

$$\overline{\phi}^x \equiv \frac{(\phi_{i-1/2} + \phi_{i+1/2})}{2} \tag{12}$$

$$\overline{\phi}^z \equiv \frac{(\phi_{k-1/2} + \phi_{k+1/2})}{2} \tag{13}$$

$$\delta_x \phi \equiv \phi_{i+1/2} - \phi_{i-1/2} \tag{14}$$

$$\delta_z \phi \equiv \phi_{k+1/2} - \phi_{k-1/2} \tag{15}$$

Here, L_z and L_x are the horizontal and vertical lengths of cell boundaries, respectively. $V_{p'}$, $V_{\rho u}$, and $V_{\rho w}$ are areas of the scalar cells, ρu cells and ρw cells, respectively. When the cells are not cut by slopes, L_z and L_x are equal to the horizontal and vertical resolutions of the model, Δx and Δz, respectively,

DOI: 10.1002/asl

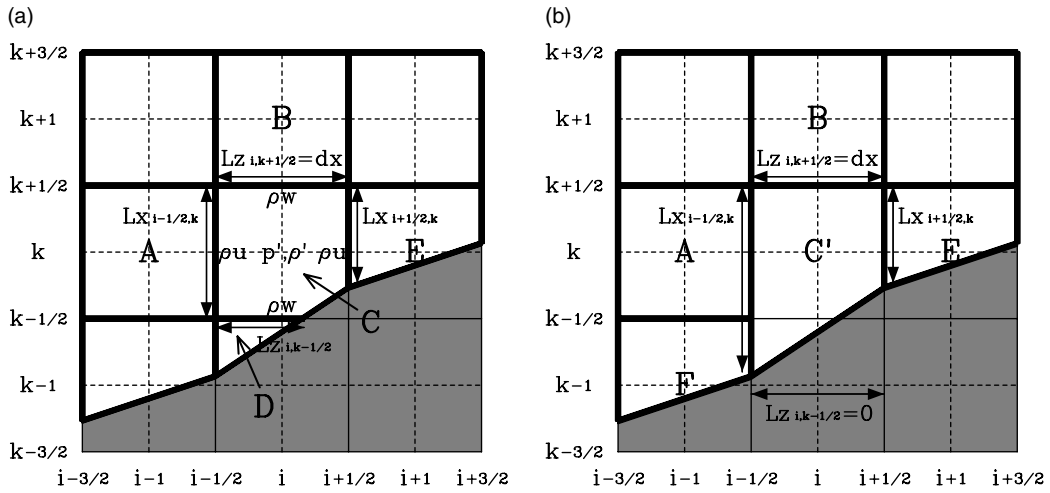

Figure 2. Combination of small cells. Thick lines describe the boundaries of the scalar cells. Shaded regions represent topography in the model. (a) Scalar cells before combination. Scalar cell C exchanges flux with the cells, A, B, D, and E. (b) Scalar cells after combining cells C and D. Combined cell C′ exchanges flux with cells A, B, E, and F.

and the cell area is equal to $\Delta x \Delta z$. The boundary lengths L_x, L_z, and the cell area are zero when the cell is completely below the slope. The leap-frog scheme with the Asselin filter (Asselin, 1972) is used for time integration.

Shaved cells such as cell D in Figure 2(a) have small areas and require small-time steps to satisfy the CFL condition. To avoid a significant increase in the computation time, cells with areas smaller than $\Delta x \Delta z/2$ are combined with the upper cells. In case of Figure 2(a), scalar cell D is combined with the upper cell C, and Figure 2(b) defines the new cell C′. The ρu cell and the ρw cell are also combined with each upper cell. The new cell C′ exchanges flux with scalar cells A, B, E, and F. This combination process does not alter the model conservation characteristics. After the combinations, we can use time steps up to half the size of the full time step for a regular cell. For example, some cells have areas less than $\Delta x \Delta z/20$ in the test of flow over a bell-shaped mountain in the next section, if the vertical combinations are not applied. Therefore, the vertical combinations make it possible to use about ten times larger time steps than those without the vertical combinations.

3. Results

Two-dimensional numerical simulations of flow over a bell-shaped mountain and a semicircular mountain are performed using the model with the V-CSC method as well as the model using the terrain-following coordinates (Satomura, 1989). Both mountains are located at the center of the domain, x_0. A sponge layer is placed higher than 15 km to avoid the gravity wave reflection at the rigid top boundary of the domain. The lower and lateral boundary conditions are free-slip and cyclic, respectively. The constant horizontal velocity, $U = 10$ m s^{-1}, is initially imposed on the entire domain. The constant Brunt–Väisälä frequency is $N = 0.01$ s^{-1}.

The surface height of the bell-shaped mountain is described as

$$z_s = \frac{h}{1 + (x - x_0)^2/a^2} \tag{16}$$

where h is the height of the mountain and a is the half-width of the mountain. Here, $h = 100$ m and $a = 5$ km are used. The horizontal resolution is 1 km and the vertical resolution is 50 m. The domain consists of 2000 and 500 cells in the horizontal and vertical directions, respectively.

The radius of the semicircular mountain is 1 km. In this case, the horizontal resolution is 250 m and the vertical resolution is 500 m. The domain consists of 2000 and 50 cells in the horizontal and vertical directions, respectively.

Figure 3(a) and (c) shows the vertical velocity fields over the bell-shaped mountain calculated by V-CSC and the terrain-following model, respectively. The vertical velocity calculated by V-CSC agrees well with that by the terrain-following model. Figure 3(b) and (d) shows the momentum flux in V-CSC and in the terrain-following model normalized by that in the linear theory, respectively. The momentum fluxes in V-CSC and in the terrain-following model are nearly unity, and agree well with that of the linear theoretical value. Figure 4(a) and (b) depicts the vertical velocity fields in the case of the semicircular mountain calculated by V-CSC and by the terrain-following model, respectively. Referring to the smooth streamlines of the analytical solution for flow over a semicircular mountain (Miles and Huppert, 1968), it is clear that mountain waves reproduced by V-CSC are more accurate than those reproduced by the terrain-following model, because the vertical velocity fields in V-CSC are clearly less noisy than those in the terrain-following model.

DOI: 10.1002/asl

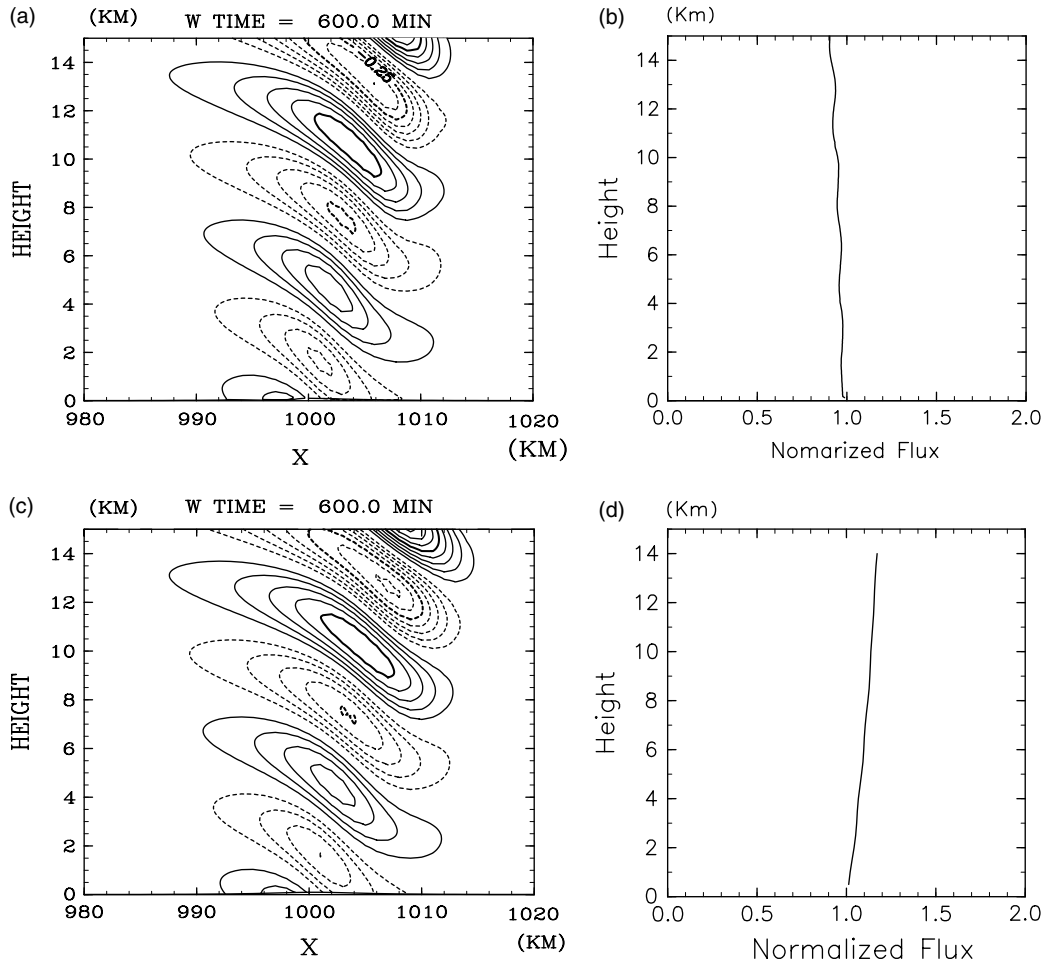

Figure 3. Vertical velocity and momentum flux over a bell-shaped mountain after integrating for 600 min: (a) vertical velocity reproduced by the vertically combined shaved cell model; (b) normalized momentum flux simulated by the vertically combined shaved cell model; (c) vertical velocity reproduced by the terrain-following model; (d) normalized momentum flux simulated by the terrain-following model. Contour intervals in (a) and (c) are 0.05 m s^{-1}. Solid and dashed lines in (a) and (c) indicate positive and negative values, respectively.

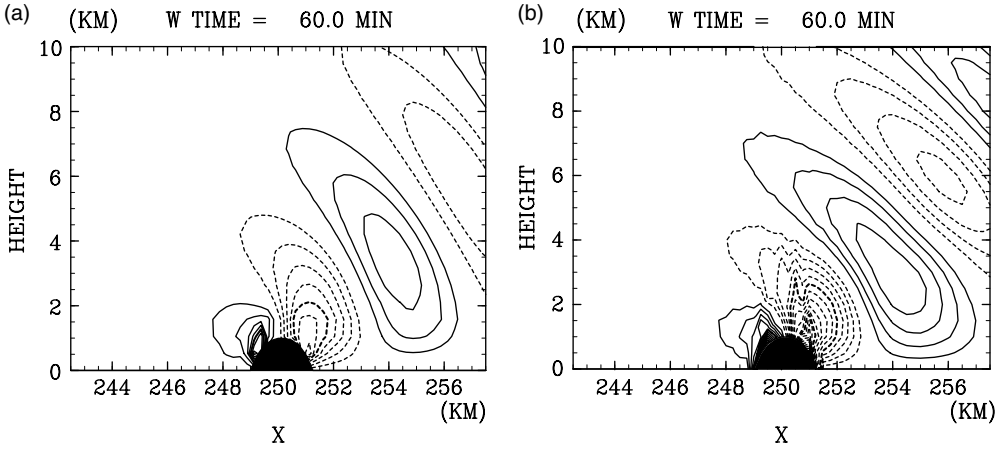

Figure 4. Vertical velocity over a semicircular mountain after integrating for 60 min (a) in the vertically combined shaved cell model, and (b) in the terrain-following model. Contour intervals are 1 m s^{-1}. Solid and dashed lines indicate positive and negative values, respectively.

Therefore, we conclude that the dynamics and the topography representation of the method proposed in this study are appropriate and sufficiently accurate for simulations of flow over complex terrain.

4. Conclusion

To achieve high-resolution and highly precise simulations over topography, the V-CSC method

DOI: 10.1002/asl

for the z-coordinate topographic representation was implemented into a nonhydrostatic atmospheric model. The solutions of flow over a bell-shaped mountain and a semicircular mountain show that the method reproduces smooth and accurate mountain waves over gentle and steep slopes. Because the z-coordinate representations do not suffer from truncation errors due to the steepness of slopes, they are well suited for high-resolution simulations where steep slopes may appear in models.

Although the shaved cell method in the original form makes small cells cut by the terrain surface, which requires small-time steps and thus large computational resource consumption to satisfy the CFL condition, the V-CSC method used in this study is a method with both sufficient accuracy and reasonable computer resource consumption.

Acknowledgements

Part of this study was supported by the Category 7 of MEXT RR2002 project for Sustainable Coexistence of Human, Nature and the Earth. Figures are drawn by the GFD-DENNOU Library.

References

Adcroft A, Hill C, Marshall J. 1997. Representation of topography by shaved cells in a height coordinate ocean model. *Monthly Weather Review* **125**: 2293–2315.

Arakawa A, Lamb VR. 1977. Computational design of the basic dynamical processes of the UCLA general circulation model. *Methods in Computational Physics* **17**: 174–267.

Asselin R. 1972. Frequency filter for time integrations. *Monthly Weather Review* **100**: 487–490.

Bonaventura L. 2000. A semi-implicit semi-Lagrangian scheme using the height coordinate for a nonhydrostatic and fully elastic model of atmospheric flows. *Journal of Computational Physics* **158**: 186–213.

Gallus W, Klemp J. 2000. Behavior of flow over step orography. *Monthly Weather Review* **128**: 1153–1164.

Mesinger F, Janjic Z, Nickovic S, Gavrilov D, Deaven D. 1988. The step-mountain coordinate: model description and performance for cases of alpine lee cyclogenesis and for a case of an Appalachian redevelopment. *Monthly Weather Review* **116**: 1493–1518.

Miles JW, Huppert HE. 1968. Lee waves in a stratified flow. Part 2. Semi-circular obstacle. *Journal of Fluid Mechanics* **33**: 803–814.

Quirk JJ. 1994. An alternative to unstructured grids for computing gas dynamic flows around arbitrarily complex two-dimensional bodies. *Computers & Fluids* **23**(1): 125–142.

Satomura T. 1989. Compressible flow simulations on numerically generated grids. *Journal of the Meteorological Society of Japan* **67**: 473–482.

Satomura T, Akiba S. 2003. Development of high-precision nonhydrostatic atmospheric model (1): Governing equations. *Annuals of Disaster Prevention Research Institute, Kyoto University* **46B**: 331–336, Links: http://www.dpri.kyoto-u.ac.jp/dat/nenpo/no46/46b0/a46b0t32.pdf.

Semtner AJ Jr, Mintz Y. 1977. Numerical simulation of the Gulf Stream and mid-ocean eddies. *Journal of Physical Oceanography* **7**: 208–230.

Steppeler J, Bitzer HW, Minotte M, Bonaventura L. 2002. Nonhydrostatic atmospheric modelling using a z-coordinate representation. *Monthly Weather Review* **130**: 2143–2149.

Steppeler J, Bitzer HW, Janjic Z, Schättler U, Prohl P, Gjertsen U, Torrisi L, Parfinievicz J, Avgoustoglou E, Damrath U. 2006. Prediction of clouds and rain using a z-coordinate nonhydrostatic model. *Monthly Weather Review* **134**: 3625–3643.

Thompson JF, Warsi ZUA, Mastin CW. 1985. *Numerical Grid Generation: Foundations and Applications*. Elsevier Science Publishing Company: North-Holland.

DOI: 10.1002/asl